Liquid Crystals

Publication details, including instructions for authors and subscription information:
http://www.informaworld.com/smpp/title~content=t713926090

Banana-shaped side chain liquid crystalline siloxanes

Remko Achten[a]; Arie Koudijs[a]; Marcel Giesbers[a]; R. Amaranatha Reddy[b]; Ton Verhulst[c]; Carsten Tschierske[b]; Antonius T. M. Marcelis[a]; Ernst J. R. Sudhölter[a]
[a] Laboratory of Organic Chemistry, Wageningen University, 6703 HB Wageningen, The Netherlands [b] Institute of Organic Chemistry, Martin-Luther-University Halle-Wittenberg, 06120 Halle (Saale), Germany [c] Philips Electronics Nederland B. V., Prof. Holstlaan 4 (WY51), 5656 AA Eindhoven, The Netherlands

To cite this Article Achten, Remko , Koudijs, Arie , Giesbers, Marcel , Reddy, R. Amaranatha , Verhulst, Ton , Tschierske, Carsten , Marcelis, Antonius T. M. and Sudhölter, Ernst J. R.(2006) 'Banana-shaped side chain liquid crystalline siloxanes', Liquid Crystals, 33: 6, 681 — 688

To link to this Article: DOI: 10.1080/02678290600682102

URL: http://dx.doi.org/10.1080/02678290600682102

Liquid Crystals, Vol. 33, No. 6, June 2006, 681–688

Taylor & Francis
Taylor & Francis Group

Banana-shaped side chain liquid crystalline siloxanes

REMKO ACHTEN†, ARIE KOUDIJS†, MARCEL GIESBERS†, R. AMARANATHA REDDY‡, TON VERHULST§, CARSTEN TSCHIERSKE‡, ANTONIUS T. M. MARCELIS*† and ERNST J. R. SUDHÖLTER†

†Laboratory of Organic Chemistry, Wageningen University, Dreijenplein 8, 6703 HB Wageningen, The Netherlands
‡Institute of Organic Chemistry, Martin-Luther-University Halle-Wittenberg, Kurt-Mothes-Str.2, 06120 Halle (Saale), Germany
§Philips Electronics Nederland B. V., Prof. Holstlaan 4 (WY51), 5656 AA Eindhoven, The Netherlands

(*Received 7 December 2005; accepted 2 February 2006*)

Eight banana-shaped side chain liquid crystalline oligomers and polymers have been synthesized by hydrosilylation of vinyl-terminated bent-core mesogens with trimethylsilyl-terminated siloxanes. The synthesized oligomers and polymers, and their olefinic precursors, were investigated by polarizing optical microscopy (POM), differential scanning calorimetry, X-ray diffraction (XRD), electro-optical experiments and Maldi-Tof. The short-tailed olefins form a $\mathrm{Col_r}$ mesophase, whereas those with longer chains exhibit the $\mathrm{SmCP_A}$ mesophase. All the oligomers and polymers studied show liquid crystalline properties and do not crystallize upon cooling. Most oligomers with around four repeating siloxane units, show a lamellar (layer) structure and antiferroelectric switching properties, the $\mathrm{SmCP_A}$ phase. XRD shows that the layer spacings are hardly influenced by the length of the terminal tails. The oligomer prepared from the smallest olefinic precursor, having the shortest alkyl tail, shows an XRD pattern reminiscent of a columnar phase, although POM displays domains of opposite chirality, and no switching behaviour could be detected. The polymers with around 35 repeating siloxane units are liquid crystalline, but due to their high viscosity a thorough characterization of the liquid crystalline phases was impossible.

1. Introduction

One of the most exciting developments in liquid crystal research in the past few years has been the discovery of (anti)ferroelectricity in liquid crystals with a non chiral bent-core or banana-shaped molecular structure, by Niori *et al*. [1]. Of all known 'banana' phases [2–8] the smectic B_2 phase, now designated as the SmCP phase, is the most interesting. Both ferroelectric and antiferroelectric ground states have been observed in this phase. In combination with two states of clinicity, four different types of layer organization can be distinguished. Depending on the molecular structure, all four sub-phases have been observed: $\mathrm{SmC_AP_A}$, $\mathrm{SmC_AP_F}$, $\mathrm{SmC_SP_A}$ and $\mathrm{SmC_SP_F}$ [3]. A related mesophase, designated as the B_7 phase, is a polarization modulated layer structure which is derived from the $\mathrm{SmC_SP_F}$ phase [7]. The exact nature of this phase is still under discussion however [9].

Due to their relatively high transition temperatures and poor processability, low molar mass banana-mesogens might become more appealing if incorporated in a polymeric system. Nevertheless, only very few attempts to polymerize bent-shaped compounds have been made [10–14]. In almost all reported cases the mesogens of the banana-shaped monomers have two polymerizable groups that are crosslinked into a polymer network. The azomethine polymers containing banana-shaped mesogens, synthesized by Choi *et al*. [10], showed B_2 properties, but due to the high viscosity the switching properties could not be investigated. Barberá *et al*. [11] were the first to prove that via *in situ* photopolymerization of banana-shaped bisacrylates SmCP networks were created. The first side chain polymer with incorporated bent-core mesogens was reported by Keith *et al*. [15]. To avoid highly viscous materials a polysiloxane copolymer was used in which the banana-shaped mesogens were strongly diluted.

In contrast to most low molar mass bent-core molecules, with an antiferroelectric ground state [16, 17], banana compounds with siloxane [15, 18–20] or carbosilane [21] groups attached, tend to show a ferroelectric organization due to a microsegregation of the three incompatible units [8]. The typical optically isotropic textures with domains of opposite handedness is often observed for bent-core molecules with siloxane segments. The optical isotropy seems to arise from a strongly deformed layer structure, where smectic slabs

---

*Corresponding author. Email: ton.marcelis@wur.nl

Liquid Crystals
ISSN 0267-8292 print/ISSN 1366-5855 online © 2006 Taylor & Francis
http://www.tandf.co.uk/journals
DOI: 10.1080/02678290600682102

are organized randomly in space. The origin of the chiral domains is not yet clear. It seems that this is *not* due to formation of a helical superstructure, as initially proposed [20]. Presently, there are at least two models under discussion. Chirality might arise from a deracemization of molecular conformers in the confined geometry of the polar layers [8] or alternatively, it might be due to the intrinsic chirality of the layers themselves [22]. This chirality is a result of the tilted organization of the molecules in polar layers, where layer normal, tilt direction and polar direction describe either a right handed or left handed system [3]. It was suggested that this inherent chirality becomes detectable if the mesophase itself is non-birefringent [22].

In this paper we present new banana-shaped side chain liquid crystal siloxane oligomers and polymers. The trimethylsilyl terminated siloxanes, contain x methylhydrosiloxane units with $x{\sim}4$ (oligomers) or $x{\sim}35$ (polymers). The compounds were synthesized by hydrosilylation of mono-unsaturated banana-shaped compounds, and their liquid crystalline properties were investigated.

2. Experimental

2.1. *Synthesis*

The synthesis of the olefinic precursors *ma*-**P**-*n* is described elsewhere [23]. All polymers were prepared by a hydrosilylation reaction (see scheme 1). Two poly(methylhydrosiloxane) backbones were used as received, a short oligomer mixture (Aldrich, $M_n{\sim}390$, $x{\sim}3.8$) and a longer oligomer mixture (Aldrich, $M_n{\sim}1700$–3200, $x{\sim}35$).

The poly(methylhydrosiloxane) backbone (Aldrich) and olefinic precursor *ma*-**P**-*n* (10 mol% excess with respect to the number of Si–H groups in the polymer backbone) were dissolved in dry toluene (~0.2 mmol *m*a-**P**-*n* per 10 ml toluene). The solution was heated to 80°C under N_2 and platinum(0)-1,3-divinyl-1,1,3,3-tetramethyl disiloxane complex (Aldrich; Karstedt catalyst, 0.1 M in xylenes) in xylenes (was added; ~2 µl per 10 ml toluene). This solution was heated under reflux for 24 h; the solvent was then evaporated under reduced pressure and the crude product purified by column chromatography on silica gel (eluant: $CH_2Cl_2 \rightarrow 2\%$ THF in CH_2Cl_2). This procedure separated the oligomers from unreacted olefinic precursor and catalyst. The composition of the oligomers was investigated by ^{1}H NMR and Maldi-Tof MS.

2.2. *Measurements*

Transition temperature measurement and optical inspection of the liquid crystalline phases were performed on samples between ordinary glass slides using an Olympus BH-2 polarizing optical microscope (POM) equipped with a Mettler FP82HT hot stage, which was controlled by a Mettler FP80HT central processor. Differential scanning calorimetry (DSC) thermograms were obtained on a Perkin Elmer DSC-7 system using 2–4 mg samples in 50 µl sample pans at a scan rate of 5°C min^{-1}. ΔH is calculated in kJ mol^{-1} for the olefinic precursors and in J g^{-1} for the oligomers/polymers. Temperature dependent X-ray diffraction (XRD) curves of the liquid crystals were measured on a Panalytical X'pert Pro diffractometer equipped with an Anton Paar camera for temperature control. For the

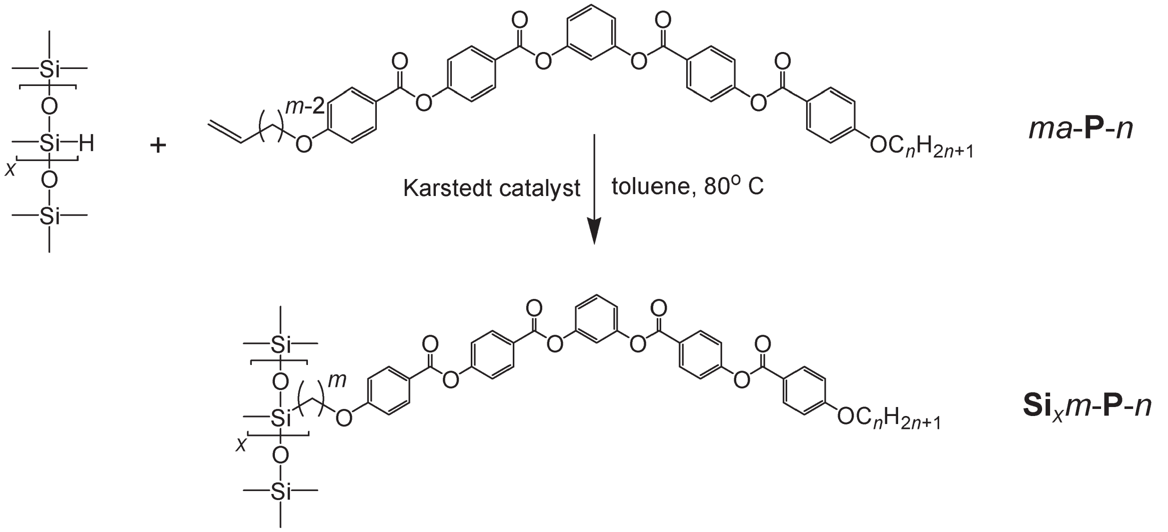

Scheme 1. Synthetic pathway for the compounds in series **Si**$_x$*m*-**P**-*n*.

measurements in the small angle region the sample was spread in the isotropic or the liquid crystalline phase on a thin glass slide (about 15 µm thick), which was placed on a temperature-regulated flat copper sample stage. The switching behaviour was determined using the triangular wave method with a 6 µm polyimide coated ITO cell, and the cells were filled in the isotropic state. Electro-optical measurements were carried out using a combination of function synthesizer (Keithley, model 3910), amplifier (Krohn-Hite, model 7500), and the current response traces were recorded using an oscilloscope (Hewlett Packard, model 54610A) across a 5 kΩ resistance. The matrix-assisted laser desorption/ionization time of flight mass spectrometer (Maldi-Tof MS) mass spectrum for compound **Si**$_{3.8}$11-**P**-12 was obtained on an Ultraflex spectrometer using 2,5-dihydroxybenzoic acid (DHB; Sigma-Aldrich) as a matrix.

3. Results and discussion

3.1. *Olefinic precursors (ma-P-n)*

Five different olefinic precursors, all belonging to series *m*a-**P**-*n*, were used to synthesize the oligomers/polymers; 11a-**P**-8, 11a-**P**-12 and 11a-**P**-16 with a 10-undecenyloxy tail, and 10a-**P**-8 and 10a-**P**-12 with a 9-decenyloxy tail. On cooling from the isotropic phase the three olefins with the longest terminal tails (11a-**P**-12, 11a-**P**-16 and 10a-**P**-12), show a smectic focal-conic texture, typical for the SmCP$_A$ phase (B$_2$-phase) [23]. Schlieren textures were also observed for these compounds. For the short-tailed olefinic precursors (11a-**P**-8 and 10a-**P**-8), spherulitic and dendritic textures, typical for the columnar Col$_r$ phase (B$_1$ phase) [24] were observed. On increasing *n* in the series 11a-**P**-*n*, the melting points decrease and the isotropization temperatures increase (table 1). The SmCP compounds showed antiferroelectric switching properties [23] whereas the Col$_r$ phase is non-switching.

The liquid crystalline phases of the banana-shaped olefinic precursors were investigated by XRD. Compound 11a-**P**-8 showed two reflections in the small angle region at d_1=28.4 Å and d_2=25.2 Å which can be assigned to a rectangular 2D-lattice (B$_1$-type mesophase). A diffuse peak in the wide angle region indicated the liquid-like behaviour of the phase. The lattice parameters calculated from the (1,1) and (0,2) reflections were a=34.4 Å and c=50.4 Å (table 1). A rough estimation of the number of molecules per unit cell, using the calculation described by Pelz *et al.* [25], results in ~six molecules, or three per column (ribbon). The POM observations for monomer 10a-**P**-8, also point to the Col$_r$ phase. This could not however be confirmed by XRD experiments due to the monotropic nature of this mesophase.

The other olefinic precursors with the longer terminal tails (11a-**P**-12, 11a-**P**-16 and 10a-**P**-12) showed sharp first and second order reflections in the small angle region corresponding to the layer spacing. The liquid-like order within the SmCP mesophase of these compounds was proven by a diffuse wide angle scattering. The layer thickness of 11a-**P**-12 and 11a-**P**-16 was 35.4 and 38.1 Å, respectively. In all cases, a tilt angle of the molecules in the smectic layers of ~45° was calculated (assuming a bending angle of 120° of the central aromatic core).

3.2. *Oligomers (Si$_{3.8}$m-P-n)*

From the ^{1}H NMR spectra the ratio between the Si–CH$_3$ and OCH$_2$ (or C–CH$_3$) protons could be calculated for oligomers **Si**$_{3.8}$*m*-**P**-*n*. Combined with the Si–H peak that was sometimes observed, we conclude that in all five cases the backbone of the oligomers was not fully occupied (~90%). On changing the reaction conditions—temperature (60–90°C), reaction time (6–72 h), catalyst (hydrogen hexachloroplatinate (IV) hydrate), olefinic precursor to siloxane ratio (1–2.5)—we were unfortunately unable to increase the degree of substitution.

The polydisperse nature of the oligomers was analysed by measuring Maldi-Tof mass spectra of **Si**$_{3.8}$11-**P**-12 (figure 1). They show the expected signals at m/z=[M+Na]$^+$ and [M+K]$^+$. For **Si**$_{3.8}$11-**P**-12 peaks corresponding with M=2 103, 3 073, 4 044 and 5 014

Table 1. Transition temperatures (°C), transition enthalpies (kJ mol^{-1}, in square brackets), layer spacings *d* (Å), and the lattice parameters *a* and *c* (Å), of the compounds in series *m*a-**P**-*n*.

Compound	Cr	Col$_r$	SmCP$_A$	I	*d*	*a*	*c*
11a-**P**-8	• 103 [37]	(• 100.5) [16]	—	•	—	34.4	50.4
11a-**P**-12	• 91 [32]	—	• 103.5 [19]	•	35.4	—	—
11a-**P**-16	• 84 [33]	—	• 107 [21]	•	38.1	—	—
10a-**P**-8	• 106 [36]	(• 103.5) [16]	—	•	—	[a]	[a]
10a-**P**-12	• 98 [15]	—	• 102 [16]	•	34.8	—	—

[a] Could not be determined due to crystallization.

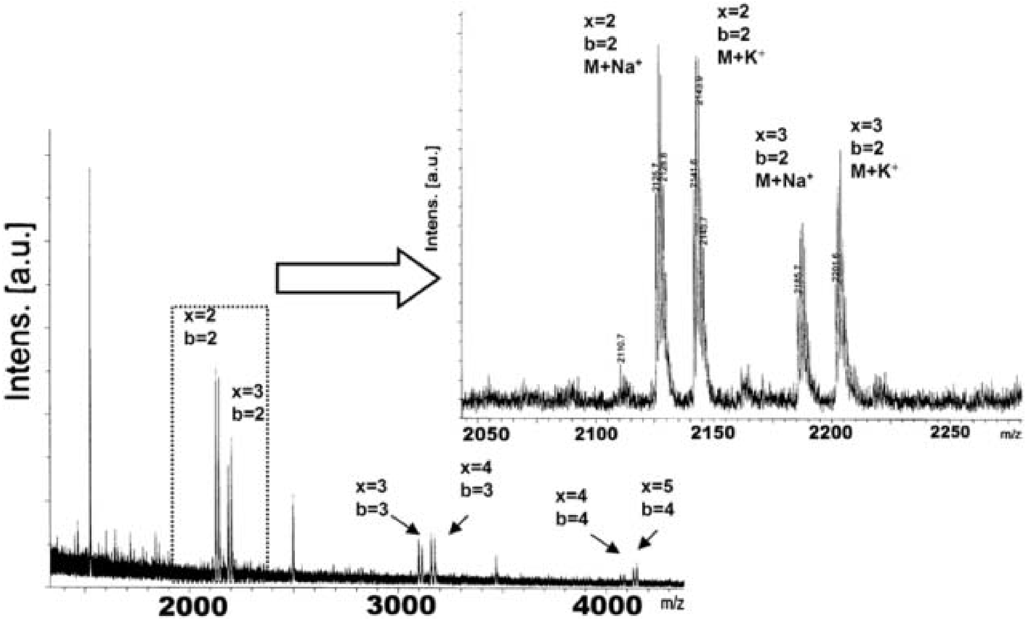

Figure 1. Maldi-Tof mass spectrum of $\mathbf{Si}_{3.8}$11-**P**-12 (b=number of olefinic precursors attached to backbone).

were observed indicating a fully occupied backbone (x=b; b=number of olefinic precursors attached to backbone) with 2, 3, 4 or 5 repeating units x. Smaller peaks corresponding with M=2 163, 3 133, 4 104 and 5 074 were observed indicating the mass of the compounds with x=3 (b=2), 4 (b=3), 5 (b=4) and 6 (b=5), with one unoccupied Si–H group. Sometimes these small Si–H signals were also observed in the ^{1}H NMR spectra. This incomplete reaction could be caused by steric hindrance by the large side chain mesogenic groups (M ranging from 841 to 967).

On cooling from the isotropic phase the POM textures of oligomers $\mathbf{Si}_{3.8}$11-**P**-*n* and $\mathbf{Si}_{3.8}$10-**P**-*n* all appear to be optically isotropic. By slightly rotating the polarizer however, regions of different brightness can be distinguished. On rotation of the polarizer in the opposite direction the brightness of the domains reverses as shown in figure 2 (i.e. the dark domains become light-coloured and the light domains become dark-coloured). This phenomenon has been observed before in siloxane-containing compounds [20, 19], and also in conventional banana-shaped compounds [24, 26–28]; as mentioned above, the origin of this chirality is not yet clear.

The isotropization temperatures of the oligomers are higher than those of the monomers. However, in contrast to the olefinic precursors the isotropization temperatures of the oligomers tend to decrease with increasing *n* (table 2). Additionally, the oligomerization seems to stabilize the lamellar SmCP structure since the

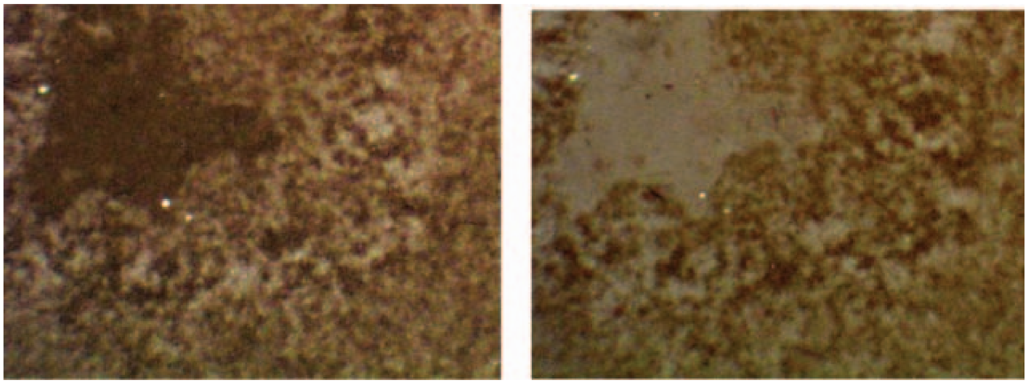

Figure 2. Optical photomicrographs obtained for the mesophase of oligomer $\mathbf{Si}_{3.8}$11-**P**-16 as seen between slightly decrossed (5–10°) polarizers in either one or the opposite direction.

Table 2. Isotropization temperatures (°C), transition enthalpies ($J\,g^{-1}$, in square brackets), and layer spacings d(Å), of the compounds in series $\mathbf{Si}_{3.8}m$-**P**-n.

Compound	$\mathrm{Col}_x^{(a)}$	$\mathrm{SmCP}_A^{(a)}$	I	d
$\mathbf{Si}_{3.8}$10-**P**-8	• 150 [19.6]		•	
$\mathbf{Si}_{3.8}$10-**P**-12		• 140 [13.8]	•	41.8
$\mathbf{Si}_{3.8}$11-**P**-8		• 150 [20.6]	•	41.7
$\mathbf{Si}_{3.8}$11-**P**-12		• 145 [20.6]	•	41.9
$\mathbf{Si}_{3.8}$11-**P**-16		• 135 [17.6]	•	42.4

[a]Indicates mesophases with chiral domains formed by achiral molecules.

columnar mesophase of monomer 11a-**P**-8 is suppressed in the corresponding oligomer $\mathbf{Si}_{3.8}$11-**P**-8. This might be due to the stronger incompatibility of the oligosiloxane units with the aromatic cores, which destabilizes the ribbon structure of the columnar phase with respect to flat layers. DSC thermograms show that the oligomers all have an additional phase transition at 70–90°C but no crystallization could be detected upon cooling the phase to room temperature. This transition leads to slightly higher d-values in the X-ray spectra, but no additional changes in XRD or POM were observed.

The switching behaviour of $\mathbf{Si}_{3.8}$11-**P**-12 was investigated using the triangular wave method. At low frequency, the apparent single polarization peak splits into two peaks (indicated by the arrow in figure 3) indicating antiferroelectric (AF) switching. On starting the switching experiments, the first threshold voltage is rather high (~200 V_{pp}); after inducing the ferroelectric (FE) state, the threshold for the switching process decreases to 100 V_{pp}. The polarization value ($\mathbf{P}_s$) is temperature dependent and has a maximum of 930 $nC\,cm^{-2}$ at ~10°C below the clearing temperature. $\mathbf{P}_s$ gradually increases upon cooling from the isotropic phase due to the relatively broad transition region (~35°C), which was also observed in the DSC-thermogram. The $\mathbf{P}_s$-value is significantly higher than for the side chain polymer described by Keith *et al.* [15] This is probably related to the dilution of the mesogenic units in the copolymer they used.

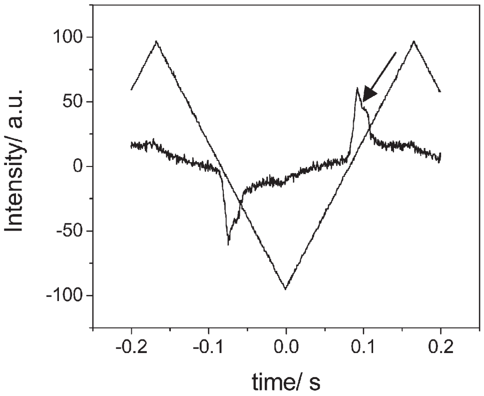

Figure 3. Switching current response trace obtained for oligomer $\mathbf{Si}_{3.8}$11-**P**-12 on applying a triangular wave voltage (200 V_{pp} for 6 μm cell thickness, at 3 Hz; temp: 100°C).

The switching process was also investigated optically on circular domains grown by slow cooling under a d.c. electrical field. The extinction crosses of the circular domains are inclined to the polarization direction of the crossed polarizers by ~45° ($\mathrm{SmC_SP_F}$) and relax to positions parallel to analyser and polarizer on terminating the applied field, which indicates the anticlinic organization of molecules in the antiferroelectric ground state (figure 4). We therefore conclude that this oligomer, as most other oligomers (table 2), exhibits the $\mathrm{SmC_AP_A}$ mesophase as ground state structure. However, in some places in the centres of these circular domains some small field-induced ferroelectric domains (synclinic) could still be seen, indicated by the arrow in figure 4 (*b*); they did not relax on removing the field. These field-induced FE domains are probably stabilized by surface interactions. Another possibility for the observ ation of these FE domains might be that a small fraction of the polydisperse oligomer mixture, with FE properties, selectively segregates from the mixture during the cooling process at the centre of the circular domains.

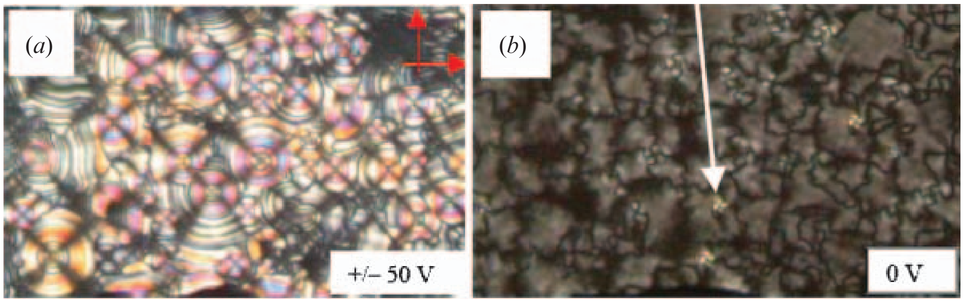

Figure 4. Optical photomicrograph of (*a*) circular domains obtained for oligomer $\mathbf{Si}_{3.8}$11-**P**-12 under a d.c. field (80 V for 6 μm cell thickness); (*b*) after relaxation on terminating the applied field. The arrow indicates a ferroelectric domain.

On application of a triangular wave electrical field up to about 350 V$_{pp}$ (5 μm cell thickness) oligomer **Si**$_{3.8}$10-**P**-8 did not show a current response. Apparently, this oligomer with the shortest terminal alkyl chain possesses a non-switchable mesophase under our experimental conditions.

Usually, banana-shaped compounds exhibit antiferroelectric switching because the AF ground state is stabilized by the escape from macroscopic polar order. The synclinic nature of the interlayer interfaces and the interlayer fluctuations resulting thereof, also play a role in the preference for an AF layer organization [8]. In microsegregated siloxane systems however, the above-mentioned interlayer fluctuations [19] are (partly) suppressed, therefore allowing a ferroelectric structure more easily [15, 18]. Nevertheless, siloxane [19, 20, 29] or carbosilane [21] systems, showing antiferroelectric mesophases, have also been reported. Reasons given in the literature for the occurrence of AF mesophases in these systems are: a small number of Si-containing segments per mesogenic group [20, 21], an even number of SiO units in dimers [19], or a large cross-sectional area of branched siloxane units which gave rise to an antiferroelectric columnar Col$_{ob}$P$_{A}$ phase [29].

In the presently described oligomers, most pairs of adjacent mesogens are also present on adjacent silicon atoms of the backbone (mesogens separated by one Si–O–Si group). These dimeric moieties could be compared with the dimers described by Dantlgraber *et al.* [19]. These dimers exhibit an odd–even effect in switching behaviour dependent on the parity of the number of Si–O units. The dimer with three Si atoms between the bananas is ferroelectric, and the dimer with four is antiferroelectric. According to the Maldi-Tof mass spectrum, the major part of oligomer **Si**$_{3.8}$11-**P**-12 has two Si atoms between the bananas (**Si**$_{3.8}$11-**P**-12, with $x=2$, $b=2$; and part of $x=3$, $b=2$; and a part of **Si**$_{3.8}$11-**P**-12, with $x \geqslant 3$). This might explain the antiferroelectric behaviour of **Si**$_{3.8}$11-**P**-12. Furthermore, the Si–O to banana ratio for **Si**$_{3.8}$11-**P**-12 is relatively low, which could also promote the antiferroelectric phases [20, 21].

On cooling from the isotropic phase, the small angle XRD patterns of oligomer **Si**$_{3.8}$11-**P**-12, show two relatively broad reflections which are indexed as (0 0 1) and (0 0 2; very weak), as shown in figure 5. The appearance of only one reflection and its second order is unusual for bent-core molecules, where usually reflections up to the fourth or sixth order can be observed. It seems that the close packing of the mesogenic units along the oligosiloxane backbone might give rise to some disorder which reduces the sharpness of the interlayer interfaces. The layer spacing was calculated to be 41.9 Å. The two other oligomers with a C$_{11}$ spacer, **Si**$_{3.8}$11-**P**-8 and **Si**$_{3.8}$11-**P**-16, exhibit very similar XRD patterns. The layer thickness of all three oligomers in the **Si**$_{3.8}$11-**P**-*n* series was barely temperature dependent. The layer spacing d increases only slightly with increasing tail length (from 41.7 to 41.9 to 42.4 Å for $n=8$, 12 and 16 respectively, table 2). The thickness of these oligomer smectic layers is significantly larger than those of the corresponding olefinic precursors. This could be expected since the siloxane backbone has a thickness of ~7 Å.

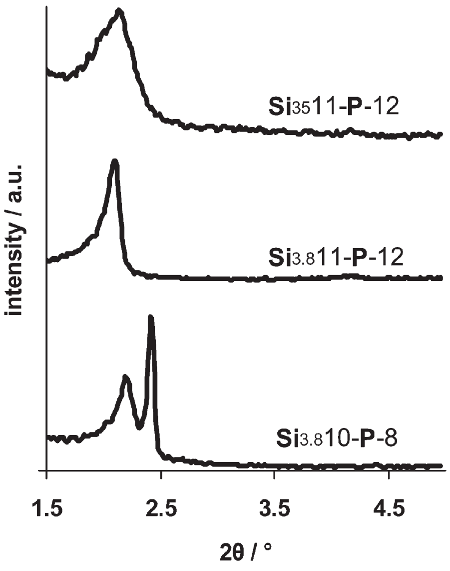

Figure 5. XRD pattern for oligomers **Si**$_{3.8}$10-**P**-8, **Si**$_{3.8}$11-**P**-12, and polymer **Si**$_{35}$11-**P**-12, all recorded at 100°C.

It seems that due to the stacking of the central aromatic part of the bananas a microsegregated system can exist which consists of a siloxane backbone segment, an aliphatic spacer/tail segment, and an aromatic segment. To a certain extent the layer thickness d is dependent only on the spacer length m. It has to be noted however that the influence of m also seems relatively small (**Si**$_{3.8}$10-**P**-12 versus **Si**$_{3.8}$11-**P**-12). Upon further cooling the SmCP phase, the transition to the low temperature phase (70–90°C) could be detected as a small increase in d-spacing.

Furthermore, the rather broad shape of the layer reflections is remarkable. This could be due to a strongly distorted structure of the smectic layers where the correlation length of the smectic slabs is significantly smaller than the wavelength of visible light (POM observations). This is in accord with the proposed disordered structure of these smectic phases.

Oligomer **Si**$_{3.8}$10-**P**-8 with a slightly shorter, even numbered, spacer between the aromatic core and the oligosiloxane unit shows a different XRD pattern from the other oligomers, with one broad and an additional

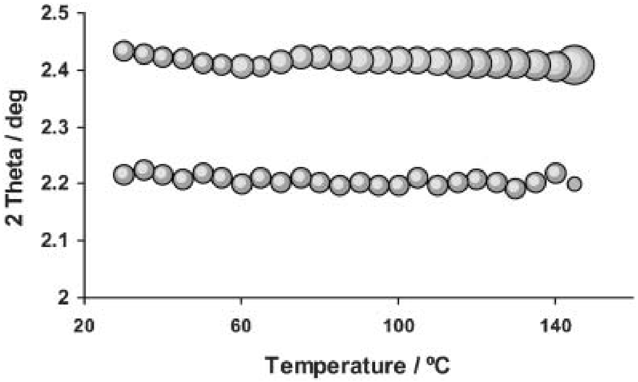

Figure 6. Temperature dependent XRD reflections of oligomer **Si**$_{3.8}$10-**P**-8 (intensity indicated by the circle size) on cooling from the isotropic phase.

relatively sharp reflection (figure 5). From figure 6, which shows the two reflections plotted against the temperature, the low temperature phase transition of the oligomer at ~70°C can be detected. This transition was also observed in the DSC thermogram at ~70°C upon cooling. The XRD pattern could indicate the presence of a mesophase with a 2D lattice. However, due to the presence of only two reflections a more precise assignment was not possible. This mesophase could be a modulated smectic phase, in which the modulation could be due to the different size of the siloxane and aliphatic segments of these systems or due to an escape from polar order. An undulated (sinusoidal deformed) smectic phase with an undulation period of about 114 Å could also be a possibility. The fact that no switching was observed points to a modulated smectic (i.e. columnar) phase driven by an escape from polar order. This would also be in accord with the fact that a columnar phase is found for its olefinic precursor 10a-**P**-8.

Additionally, and this is most remarkable, this phase is optically isotropic and shows chiral domains while, normally, columnar phases are birefringent. There is no previous report of a columnar phase with a dark conglomerate texture, but Pelzl *et al.* [9] have reported a B_7 phase with an oblique cell, which was formed upon cooling from a high temperature smectic phase with dark textures, explaining the dark texture in the B_7 phase at lower temperature (paramorphotic texture). However, in the presently investigated oligomer no high temperature smectic phase could be detected that could similarly induce dark textures in the low temperature columnar phase. It seems that this new mesophase with a 2D lattice is a modulated variant of the dark conglomerate smectic phases. In this case, the optical activity might be due to the superstructural layer chirality within the modulated layers, which becomes visible in the optically isotropic mesophase [22]. On the other hand, a deracemization of chiral (helical) conformers in the confined geometry of the smectic ribbons could lead to chirality in the ribbons which could probably also lead to a chirality-induced distortion of the ribbons [8].

So, although the exact structure of the mesophases of **Si**$_{3.8}$10-**P**-8 is unclear, a simple smectic structure can be excluded and therefore this unknown non-switchable modulated smectic (i.e. columnar) phase is designated as Col$_x^{(a)}$.

3.3. *Polymers(Si$_{35}$m-P-n)*

As with the oligomers with the short backbone, not all Si–H groups of the longer siloxanes (x~35) reacted with a banana-shaped olefinic precursor. According to the ^{1}H NMR spectrum about 70% of all available Si–H sites reacted. On cooling from the isotropic phase the polymers **Si**$_{35}$*m*-**P**-*n*, remained optically isotropic. Even after slightly rotating the polarizer no regions of different brightness could be observed. One possibility is that the chiral domains are too small to be observed under the polarizing microscope. However, it is also possible that the phase itself is achiral, as reported for another example [30]. The isotropization temperatures were determined from the DSC thermograms. Changing the length of the spacer or the terminal tail does not influence the transition temperatures significantly (table 3). All the polymers have a low temperature phase transition, similar to those observed for the oligomers. These transitions are observed at lower temperatures, however (45–60°C). We were unable to perform switching experiments since the polymers were very viscous, and could not be introduced into the cells.

The XRD patterns of polymers **Si**$_{35}$11-**P**-*n* (n=12 and 16) show weak, relatively broad reflections in the small angle region at ~42 Å (table 3, figure 5). The broad reflections are an indication of short correlation lengths, which might be caused by very small domains. This might also be the reason that no clear texture is revealed by POM. Due to the similar backbone structure and similar layer thickness as found for the oligomers, the

Table 3. Transition temperatures (°C), transition enthalpies (J g^{-1}, in square brackets), and layer spacings *d*(Å), of the compounds in series **Si**$_{35}$*m*-**P**-*n*.

Compound	SmCP	I	*d*
Si$_{35}$10-**P**-12	• 140 [8]	•	[a]
Si$_{35}$11-**P**-12	• 150 [11]	•	~41
Si$_{35}$11-**P**-16	• 155 [15]	•	~42

[a] Could not be determined.

polymers probably also have a layered organization and this could be a SmCP structure.

Our findings show that the unique properties of banana-shaped molecules can be maintained in side chain liquid crystalline oligosiloxanes. However, because of their high viscosity these materials soon become unprocessable with increasing polymer chain length. An approach employed by Keith *et al.* [15], in which siloxanes were used with a low degree of substitution, seems to be more promising.

4. Conclusions

Eight new banana-shaped side chain liquid crystalline oligomers/polymers have been synthesized and characterized. According to the ^{1}H NMR and Maldi-Tof mass spectra the backbones of the oligomers/polymers are not fully occupied and some unreacted Si–H groups are still present. The olefinic precursors all show conventional $\mathrm{Col_r}$ or $\mathrm{SmCP_A}$ mesophases. In the pure state all oligomers have an optically isotropic mesophase composed of domains of opposite chirality (dark conglomerate phases). Electro-optical investigations indicate antiferroelectric switching properties with a predominant anticlinic layer structure at zero voltage. They are therefore believed to have a distorted $\mathrm{SmC_AP_A}$ layer organization. One of the oligomers shows a non-switchable columnar phase, also composed of domains of opposite chirality, whose structure is not exactly clear. The polymers with the longer backbones exhibit an optical isotropic mesophase, without detectable chiral domains, that could not be characterized by switching experiments due to its high viscosity. Comparison of the layer spacing with the shorter oligomers indicates that a lamellar ordering is likely for these materials.

References

[1] T. Niori, F. Sekine, J. Watanabe, T. Furukawa, H. Takezoe. *J. mater. Chem.*, **6**, 1231 (1996).

[2] G. Pelzl, S. Diele, W. Weissflog. *Adv. Mater.*, **11**, 707 (1999).

[3] D.R. Link, G. Natale, R. Shao, J.E. Maclennan, N.A. Clark, E. Körblova, D.M. Walba. *Science*, **278**, 1924 (1997).

[4] D.M. Walba, E. Korblova, R. Shao, J.E. Maclennan, D.R. Link, M.A. Glaser, N.A. Clark. *Science*, **288**, 2181 (2000).

[5] M. Nakata, D.R. Link, F. Araoka, J. Thisayukta, Y. Takanishi, K. Ishikawa, J. Watanabe, H. Takezoe. *Liq. Cryst.*, **28**, 1301 (2001).

[6] J.P. Bedel, J.C. Rouillon, J.P. Marcerou, M. Laguerre, H.T. Nguyen, M.F. Achard. *Liq. Cryst.*, **28**, 1285 (2001).

[7] D.A. Coleman, J. Fernsler, N. Chattham, M. Nakata, Y. Takanishi, E. Korblova, D.R. Link, R.-F. Shao, W.G. Jang, J.E. Maclennan, O. Mondainn-Monval, C. Boyer, W. Weissflog, G. Pelzl, L.-C. Chien, J. Zasadzinski, J. Watanabe, D.M. Walba, H. Takezoe, N.A. Clark. *Science*, **301**, 1204 (2003).

[8] R. Amaranatha Reddy, C. Tschierske. *J. mater. Chem.*, **16**, 907 (2006).

[9] G. Pelzl, M.W. Schröder, U. Dunemann, S. Diele, W. Weissflog, C. Jones, D.A. Coleman, N.A. Clark, R. Stannarius, J. Li, B. Das, S. Grande. *J. mater. Chem.*, **14**, 2492 (2004).

[10] E.-J. Choi, J.-C. Ahn, L.-C. Chien, C.-K. Lee, W.-C. Zin, D.-C. Kim, S.-T. Shin. *Macromolecules*, **37**, 71 (2004).

[11] J. Barberá, N. Gimeno, L. Monreal, R. Pinol, M.B. Ros, J.L. Serrano. *J. Am. chem. Soc.*, **126**, 7190 (2004).

[12] A.C. Sentman, D.L. Gin. *Angew. Chem. int. Ed.*, **42**, 1815 (2003).

[13] C.-D. Keum, A. Kanazawa, T. Ikeda. *Adv. Mater.*, **13**, 321 (2001).

[14] G. Galli, S. Demel, C. Slugovc, F. Stelzer, W. Weissflog, S. Diele, K. Fodor-Csorba. *Mol. Cryst. liq. Cryst.*, **439**, 1909 (2005).

[15] C. Keith, R. Amaranatha Reddy, C. Tschierske. *Chem. Commun.*, 871 (2005).

[16] D. Shen, A. Pegenau, S. Diele, I. Wirth, C. Tschierske. *J. Am. chem. Soc.*, **122**, 1593 (2000).

[17] R. Achten, E.A.W. Smits, R. Amaranatha Reddy, M. Giesbers, A.T.M. Marcelis, E.J.R. Sudhölter. *Liq. Cryst.*, **33**, 57 (2006).

[18] G. Dantlgraber, U. Baumeister, S. Diele, H. Kresse, B. Lühmann, H. Lang, C. Tschierske. *J. Am. chem. Soc.*, **124**, 14852 (2002).

[19] G. Dantlgraber, S. Diele, C. Tschierske. *Chem. Commun.*, 2768 (2002).

[20] G. Dantlgraber, A. Eremin, S. Diele, A. Hauser, H. Kresse, G. Pelzl, C. Tschierske. *Angew. Chem. int. Ed.*, **41**, 2408 (2002).

[21] C. Keith, R. Amaranatha Reddy, H. Hahn, H. Lang, C. Tschierske. *Chem. Commun.*, 1898 (2004).

[22] L.E. Hough, N.A. Clark. *Phys. Rev. Lett.*, **95**, 107802 (2005).

[23] R. Achten, A. Koudijs, M. Giesbers, A.T.M. Marcelis, E.J.R. Sudhölter. *Liq. Cryst.*, **32**, 277 (2005).

[24] R. Amaranatha Reddy, B.K. Sadashiva. *Liq. Cryst.*, **30**, 1031 (2003).

[25] K. Pelz, W. Weissflog, U. Baumeister, S. Diele. *Liq. Cryst.*, **30**, 1151 (2003).

[26] J. Ortega, C.L. Folcia, J. Etxebarria, N. Gimeno, M.B. Ros. *Phys. Rev. E*, **68**, 011707 (2003).

[27] A. Jákli, Y.-M. Huang, K. Fodor-Csorba, A. Vajda, G. Galli, S. Diele, G. Pelzl. *Adv. Mater.*, **15**, 1606 (2003).

[28] J. Svoboda, V. Novotna, V. Kozmik, M. Glogarova, W. Weissflog, S. Diele, G. Pelzl. *J. mater. Chem.*, **13**, 2104 (2003).

[29] C. Keith, R. Amaranatha Reddy, U. Baumeister, C. Tschierske. *J. Am. chem. Soc.*, **126**, 14312 (2004).

[30] G. Liao, S. Stojadinovic, G. Pelzl, W. Weissflog, S. Sprunt, A. Jákli. *Elec. liq. Cryst. Commun.* (2004).